CONCURRENT MAPPING & LOCALISATION USING SIDE-SCAN SONAR FOR AUTONOMOUS NAVIGATION

I. Tena Ruiz, S. Reed, Y. Petillot, J. Bell and D. M. Lane

Ocean Systems Laboratory
Heriot-Watt University

Edinburgh, UK

Abstract

Concurrent Mapping and Localisation (CML) is a proven and well-developed tool for navigating in unknown environments. It can be used as a substitute to common absolute sensors, such as GPS or acoustic baseline systems. The Ocean Systems Laboratory (OSL) recently developed a CML system that builds a map of the environment using observations of landmarks extracted from side-scan sonar (SS). This system worked as a post-processing tool. An operator extracted the landmarks manually and matched them to existing landmarks in the CML state. The CML output was subsequently smoothed and used to create high quality, large-scale side-scan sonar mosaics. This paper extends this system by introducing automatic landmark extraction techniques and enhanced automatic data association. The automatic extraction technique used a Markov Random Field (MRF) model to detect possible landmarks in the SS images. MRF models provide a suitable framework for incorporating a priori information regarding the general appearance of landmarks in SS imagery and have been shown to work well on noisy images. Detected false alarms are subsequently removed using a Co-operating Statistical Snake model. This model requires the landmark be statistically different from the surrounding seafloor. The enhanced data association algorithm incorporates landmark descriptors, as well as the landmarks estimated position and covariance, to automatically match the observations to the existing landmark map. The resulting module could be easily integrated to an underwater platform to perform autonomous navigation.

Introduction

The current state of the art in AUV technology requires that a vehicle's navigation be aided by either acoustic baseline systems or GPS fixes on the surface. The AUV is not free to explore. It must keep close to the sea's surface for GPS fixes; or within a limited distance from a vessel equipped with either SBL or USBL; or it must remain within a region of size determined by an LBL network. Without baseline or GPS navigation the vehicle's dead-reckoning error would grow. For the AUV to explore at greater depths, without outside assistance, new methods for absolute navigation must be developed. To this end the research community has proposed the used of CML. These techniques propose to use the environment to build a map that the AUV can the use to localise itself.

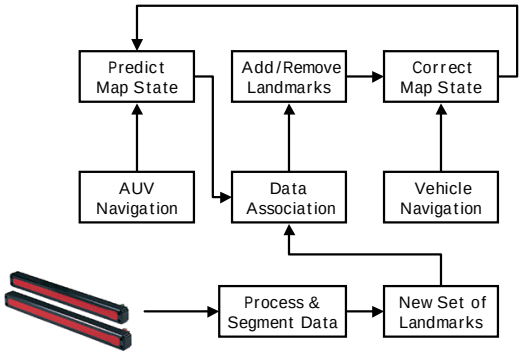

Figure 1: Overview of System

The OSL at Heriot-Watt University has been involved in this process. First proposing and demonstrating the use of forward-look sonar systems [TEN01a] and more recently developing and demonstrating systems using side-scan sonar for post-processing data [TEN03a, TEN03b]. This paper extends this work so as to also provide automatic landmark extraction and data association. Such techniques must be robustly developed if the system were to be integrated and operated in real-time. This work builds on the OSL's broad experience in Computer Aided Detection and Computer Aided Classification

[REE03a, REE03b] and landmark feature descriptors and data association algorithms [TEN99, TEN01b].

An overview of the proposed system functionality can be seen in Figure 1. This system has been implemented and tested in post-processing mode. Findings will be reported in the result section. The following sections will examine the system in detail. They will describe the CML process, the automatic landmark detection module and the data association strategy. The paper will also provide a conclusion and offer an insight into planned future work.

Concurrent Mapping & Localisation

The CML solution proposed in this paper was initially put forward in [SMI90]. This technique, known in some of the literature as the stochastic map, has been successfully implemented by the OSL to perform CML using forward-look sonar [TEN01b]. This solution proposes an augmentation of the extended Kalman filter [MAY82]. The filter now holds the relevant states of the vehicle and that of the landmarks used in the mapping and localisation process. The new state vector $\mathbf{x}(\cdot)$ assumes the following form,

$$\mathbf{x}(k) = [\mathbf{x}_v(k) \quad \mathbf{x}_1(k) \quad \mathbf{x}_2(k) \quad \cdots \quad \mathbf{x}_n(k)]^T \quad (1)$$

The estimated error covariance for this system,

$$\mathbf{P}(k) = \begin{bmatrix} \mathbf{P}_{vv}(k) & \mathbf{P}_{v1}(k) & \cdots & \mathbf{P}_{vn}(k) \\ \mathbf{P}_{1v}(k) & \mathbf{P}_{11}(k) & \cdots & \mathbf{P}_{1n}(k) \\ \vdots & \vdots & \ddots & \vdots \\ \mathbf{P}_{nv}(k) & \mathbf{P}_{n1}(k) & \cdots & \mathbf{P}_{nn}(k) \end{bmatrix} \quad (2)$$

The state is propagated using the standard extended Kalman filter equations; i.e. assuming that the process and observation models are locally linear, and that the process and observation noise is small. The new state vector and associated covariance are thus,

$$\hat{\mathbf{x}}(k) = \mathbf{f}[\hat{\mathbf{x}}(k-1), \mathbf{u}(k), \mathbf{0}, k] \quad (3)$$

$$\mathbf{P}(k) = \nabla\mathbf{f}_v \mathbf{P}(k) \nabla\mathbf{f}_v{}^T + \nabla\mathbf{f}_w \mathbf{Q}(k) \nabla\mathbf{f}_w{}^T \quad (4)$$

The filter can now be updated according to,

$$\hat{\mathbf{x}}(k+1) = \hat{\mathbf{x}}(k) + \mathbf{K}(k)\upsilon(k) \quad (5)$$

$$\mathbf{P}(k+1) = \mathbf{P}(k) - \mathbf{K}(k)\mathbf{H}(k)\mathbf{P}(k) \quad (6)$$

where the innovation is,

$$\upsilon(k) = \mathbf{z}(k) - \mathbf{h}[\hat{\mathbf{x}}(k+1 \mid k), \mathbf{0}, k] \quad (7)$$

its covariance,

$$\mathbf{S}(k) = \mathbf{H}(k)\mathbf{P}(k)\mathbf{H}^T(k) + \mathbf{R}(k) \quad (8)$$

and the filter gain,

$$\mathbf{K}(k) = \mathbf{P}(k)\mathbf{H}^{\mathbf{T}}(k)\mathbf{S}^{-1}(k) \quad (9)$$

The observation vector adopted to incorporate side-scan data is as follows:

$$\mathbf{z}_i(k) = [a \quad b]^T \quad (10)$$

where a is the cross-track distance obtained after slant-range correcting the side-scan sonar return, b is the along-track distance computed using the pitch and the altitude of the vehicle. The prediction vector will therefore be:

$$\hat{\mathbf{z}}_i(k) = \begin{bmatrix} \bar{x}_i(k)\cos\theta_v(k) - \bar{y}_i(k)\sin\theta_v(k) \\ \bar{x}_i(k)\sin\theta_v(k) + \bar{y}_i(k)\cos\theta_v(k) \end{bmatrix} \quad (11)$$

where $\bar{x}_i(\cdot)$ and $\bar{y}_i(\cdot)$ are the predicted landmark coordinates and $\theta_v(\cdot)$ is the predicted vehicle's heading.

The vehicle will not be able to observe all landmarks during each update. Those that are observed must be associated to the landmarks in the stochastic map state vector $\mathbf{x}(k)$. This is known as data association. Data association has been a subject of major research. The data

association process will be examined later in the document. Observations that were not associated to an existing landmark will be added to the stochastic map state and covariance. The new map state and associated covariance will be

$$\hat{\mathbf{x}}(k) \leftarrow \begin{bmatrix} \hat{\mathbf{x}}(k) \\ \hat{\mathbf{x}}_{n+1}(k) \end{bmatrix} \quad (12)$$

$$\begin{aligned} \mathbf{P}_{n+1n+1}(k) &= \mathbf{L}_{x_v}\mathbf{P}_{vv}(k)\mathbf{L}_{x_v}{}^T + \mathbf{L}_{z_{new}}\mathbf{R}(k)\mathbf{L}_{z_{new}}{}^T \\ \mathbf{P}_{n+1v} &= \mathbf{P}_{vn+1}{}^T(k) = \mathbf{L}_{x_v}\mathbf{P}_{vv}(k) \end{aligned} \quad (13)$$

Automatic Landmark Detection

The Segmentation Process

Markov Random Field (MRF) models have been used in a variety of segmentation problems [REE03c] due to their ability to consider spatial information and model a priori information. The model described here segments raw sonar images into regions of object-highlight, shadow and background. Landmarks appear in Sidescan imagery as a highlight/shadow pair (as seen in Figure 3 and Figure 5) producing a distinctive signature which can be modeled using priors.

A set of 3 random field Z={X,Y,O} is considered where field Y is the observed raw sidescan image and X and O are the unobservable, underlying label fields which we wish to recover. Field X={X_s,s∈S} (s denotes a pixel position on image S) contains labels e_0=shadow, e_1=sea bottom-reverberation and e_2=object-highlight while field O contains labels o_0=object and o_1=non-object. The probability of the unobservable data given field Y can be obtained using Baye's theorem

$$\begin{aligned} &P_{X,O|Y}(x,o \mid y) \propto \\ &P_X(x)P_{O|X}(o \mid x)P_{Y|X}(y \mid x) \end{aligned} \quad (14)$$

The desired underlying label fields can be obtained [REE03a] by minimizing posterior energy term

$$\begin{aligned} &U(x,y,o) = \\ &\sum_{s\in S}\Phi_s(x_s,y_s) + \sum_{<s,t>}\beta_{st}[1-\delta(x_s,x_t)] \\ &-\sum_{s\in S}\delta(x_s,e_2).\ln\Psi_X(s) - \sum_{s\in S}\chi_s(x_s,o_s) \end{aligned} \quad (15)$$

The first term on the r.h.s is the energy term relating to P(Y|X) and considers the probability of each of the classes producing greylevel y_s. The second term models the spatial dependency of label x_s on the neighbouring label field where an 8-neighbour anisotropic Potts model has been used [MIG99]. The third term models the knowledge that an object-highlight region is usually accompanied by a shadow region by using a shadow potential field to discourage pixels far from a shadow region from being labelled object-highlight. The final term ensures that only object-highlight regions of the correct size are detected. More details of this model can be found in [REE03a].

Post-Processing

In images containing complex seafloors, false alarms will be detected which should be removed. Navigational information available from the AUV can be used to determine the size and height of each of the detected object-highlight regions. Objects that have dimensions outwith an acceptable range can then be removed. A Co-operating Statistical Snake (CSS) [REE03b, REE03c] is used to extract the object-highlight and shadow regions of the remaining landmarks. This model extended the ideas in [CHE99] to include information on the correlation between the object-highlight and shadow regions to produce accurate segmentation results, even on complex seafloors. The CSS model removes detections that do not have distinctive object-highlight and shadow regions.

Detections

The model is demonstrated on 2 Sidescan sonar images. The first can be seen in Figure 2, it contains 4 objects which could be used as landmarks.

All 4 objects were detected as shown in Figure 3. Figure 3 also contains the segmentation results obtained by the CSS model for each of the detected objects. The landmark's clear object-highlight and shadow regions ensured none of the objects were labelled as false alarms and removed.

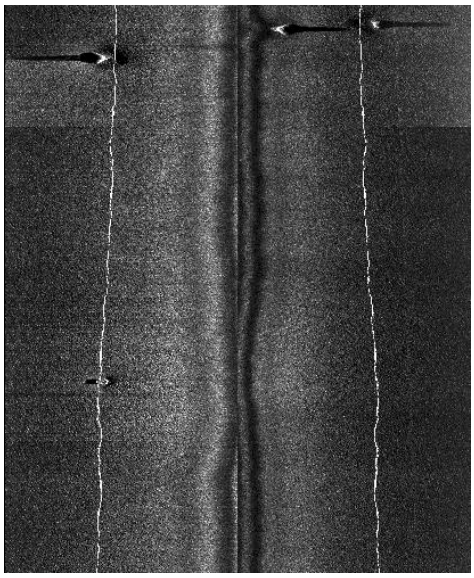

Figure 2: Raw Sidescan Image containing 4 objects.

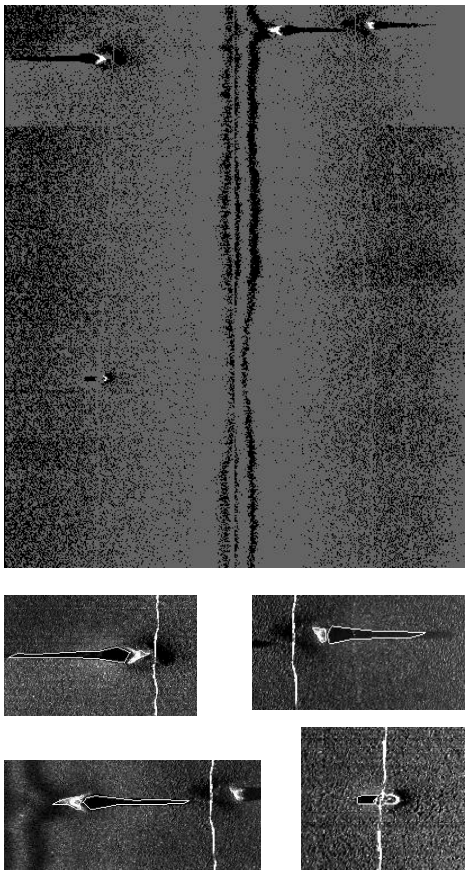

Figure 3: The final detection and feature extraction results for the raw image contained in Figure 2.

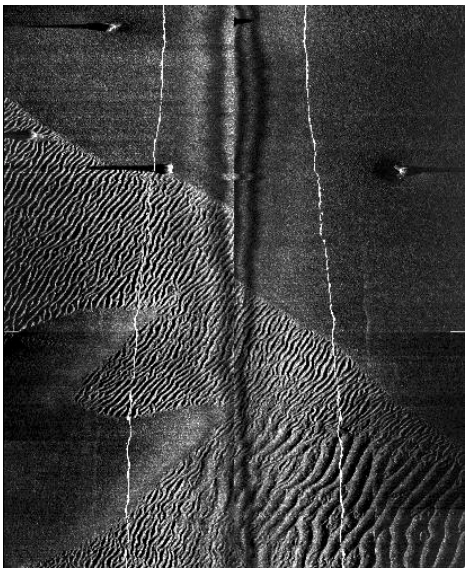

Figure 4: Raw Sidescan Image containing 4 objects. Some of the objects lie on a sand ripple seafloor making detection and feature extraction difficult.

The second image under consideration is shown in Figure 4. This shows objects lying on a sand ripple seafloor, which makes accurate shadow extraction difficult. The results are shown in Figure 5.

As Figure 5 shows, all the objects have been detected and their features extracted well. These results demonstrate how the Detection and CSS models are able to operate well on complex sonar images.

Automatic Data Association

Data association has been a subject of major research by the multiple target tracking community. A good description of various methods can be found in [BAR88]. However, a method developed with the stochastic map in mind is the *Joint Compatibility Test (JCT)* method. Proposed by Neira and Tardós [NEI00], it finds the event with the maximum number of pairings that maintains the overall consistency of the map. The *Nearest Neighbour (NN)* approach proposed by other researchers, and adapted from the multiple target literature, has ignored the joint compatibility of the pairings and failed to take into account the importance of the correlations between the landmarks. Both the JCT and NN methods have been shown to

improve their performance when aided by landmark descriptors [TEN01a, TEN01b].

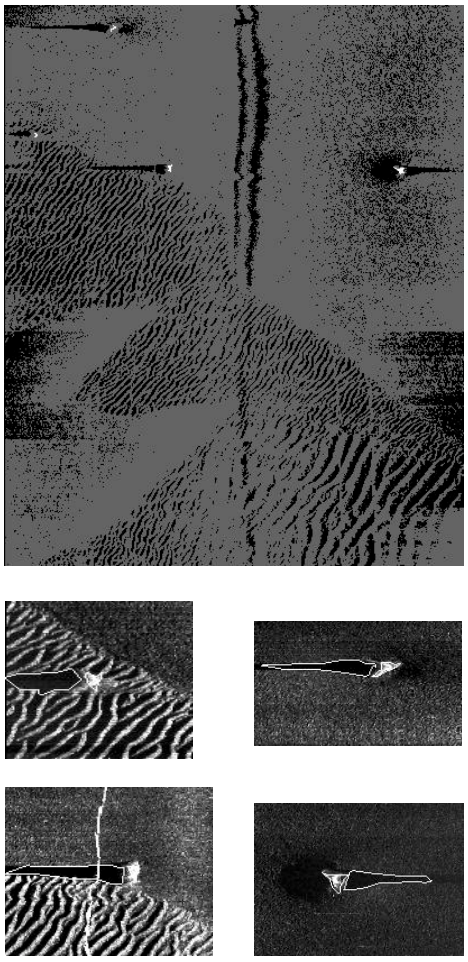

Figure 5: The detection and extraction results for Figure 4. All the objects have been detected. The shadow regions have all been well extracted even when the object lies on a ripple seafloor.

The JCT evaluates incrementally an association event $\theta\{k\}$. The association event is made up of a set of possible associations $\theta\{k\}=\{j_1, j_2, \cdots, j_i\}$ at sample period k. It is built by iteratively checking the map's consistency for each association included in the event. The compatibility test, which guarantees consistency, is the Mahalanobis distance,

$$d_i^2(k) = \mathbf{Y}_i^T \mathbf{S}_i^{-1} \mathbf{Y}_i \qquad (16)$$

where $\mathbf{Y}_i$ is the innovation vector for the association event $\theta\{k\}$

$$\mathbf{Y} = \left[\upsilon_{j_1}, \upsilon_{j_2}, \cdots, \upsilon_{j_i}\right]^T \qquad (17)$$

and $\mathbf{S}_i$ is the innovation covariance for that same event,

$$\mathbf{S}_i = \mathbf{H}_i \mathbf{P} \mathbf{H}_i^T + \mathbf{R} \qquad (18)$$

where

$$\mathbf{H}_i = \left.\frac{\partial \mathbf{h}[\mathbf{x}, i]}{\partial \mathbf{x}}\right|_{\mathbf{x}=\hat{\mathbf{x}}} \qquad (19)$$

Now for each new association, the innovation $\upsilon_{j_{i+1}}$ and corresponding covariance,

$$\mathbf{S}_{j_{i+1}} = \mathbf{H}_{j_{i+1}} \mathbf{P} \mathbf{H}_{j_{i+1}}^T + \mathbf{R} \qquad (20)$$

where

$$\mathbf{H}_{j_{i+1}} = \left.\frac{\partial \mathbf{h}[\mathbf{x}, j_{i+1}]}{\partial \mathbf{x}}\right|_{\mathbf{x}=\hat{\mathbf{x}}} \qquad (21)$$

can be used to obtain an updated Mahalanobis distance. Given,

$$\mathbf{S}_{i+1} = \begin{bmatrix} \mathbf{S}_i & \mathbf{w}_{i+1}^T \\ \mathbf{w}_{i+1} & \mathbf{S}_{j_{i+1}} \end{bmatrix} \qquad (22)$$

where

$$\mathbf{w}_{i+1} = \mathbf{H}_{j_{i+1}} \mathbf{P} \mathbf{H}_i^T \qquad (23)$$

The association event can be incrementally updated by using the partitioning method for matrix inversion [HAR97]. This method finds iteratively the inverse innovation covariance for the each new event.

In this implementation, the JCT will be aided by also using the height of the observed landmarks as a state of the landmark. The height will act as a descriptor and help the system produce accurate matches.

Results

The following results were obtained by processing data gathered during the BP'02 experiments carried out by the SACLANT Undersea Research Centre in La Spezia, Italy. The side-scan data was gathered by a REMUS AUV [ALT01]. The automatic landmark extractor found 85 possible landmarks. The JCT algorithm and the stochastic map used these landmarks to produce a new possible trajectory, see Figure 6.

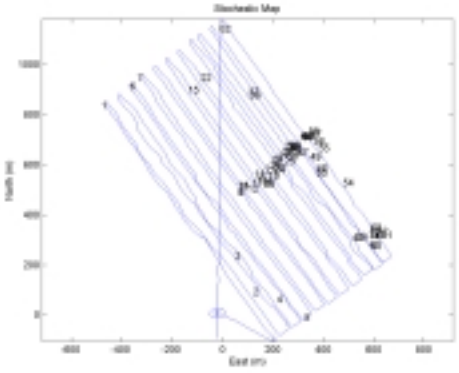

Figure 6: Resulting trajectory using automatic landmark extraction and association CML.

The new trajectory obtained using this strategy was used to produce a mosaic and it can be compared to a mosaic produced without the CML. Figure 7 zooms into the resulting mosaic produced with no CML. It can be seen how the same landmark appears in two different places, due to the errors in the navigation solution. Figure 8 shows the mosaic when CML is used.

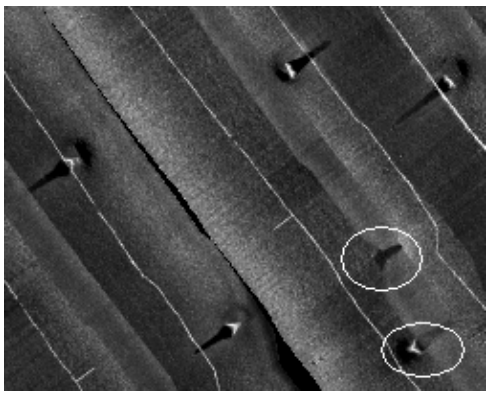

Figure 7: A mosaic produced when the landmarks have not been extracted and matched.

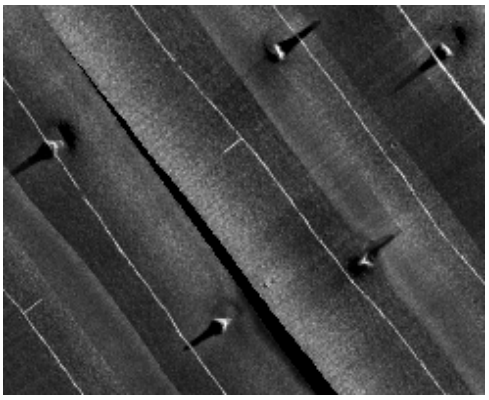

Figure 8: Mosaic produced when the landmarks are automatically extracted and matched.

Conclusion

The following paper has presented a system capable of automatically extracting landmarks and matching them to previously observed landmarks. These landmarks can be used to update a CML algorithm. The results are encouraging. These demonstrate that errors in navigation can be reduced using this system.

At this stage more experimentation is required, false alarms can adversely affect the solution and techniques for minimising these must be developed.

Acknowledgements

The authors would like to thank the SACLANT Undersea Research Centre, the US Office of Naval Research and The Woods Hole Oceanographic Institution for allowing the inclusion of data from the BP'02 experiment.

References

[BAR88] – Y. Bar-Shalom and T. E. Fortmann. Tracking and Data Association. Volume 179 141 of the Mathematics in Science and Engineering, Academic Press, 1988.

[CHE99] – C. Chesnaud, P. Refregier and V. Boulet. Statistical region snake-based segmentation adapted to different physical noise models. In IEEE Trans.Pattern Anal. Machine Intell., Vol. 21(11), pp. 1145-1157, Dec 1999.

[HAR97] – D. A. Harville. Matrix Algebra from a statistician's perspective. Springer-Verlag, New York, USA, 1997.

[MAY82] – P. S. Maybeck. Stochastic Models, Estimation, and Control, Volume 2. Volume 141 of the Mathematics in Science and Engineering, Academic Press, 1982.

[MIG99] – M. Mignotte, C. Collet, P. Perez and P. Bouthemy. Three class markovian segmentation of high resolution sonar images. In Comput. Vis. Image Und., Vol. 76(3), pp. 191-204, Dec 1999.

[NEI00] – J. Neira and J. D. Tardós. Robust and feasible data association for simultaneous localization and map building. In IEEE International Conference in Robotics and Automation, Workshop W4, Mobile Robot Navigation and Mapping, San Francisco, California, USA, April 2000.

[REE03a] – S. Reed, Y. Petillot and J. Bell. An automated approach to the detection and extraction of mine features in sidescan sonar. In IEEE Journal Oceanic Eng., vol. 28(1), pp. 90-106, Jan. 2003.

[REE03b] – S. Reed, Y. Petillot and J. Bell. A model-based approach to the detection and classification of mines in sidescan sonar. In MREP03 Conference, La Spezia, Italy, May 2003.

[REE03c] – S. Reed, Y. Petillot and J. Bell. An automated approach to the classification of mine-like objects in sidescan sonar using highlight and shadow information. Unpublished.

[SMI90] – R. Smith, M. Self and P. Cheeseman . Estimating Uncertain Spatial Relationships in Robotics. In Autonomous Robot Vehicles, Springer-Verlag, 167-193, 1990.

[TEN99] – I. Tena Ruiz, D. M. Lane, and M. J. Chantler. A comparison of inter-frame feature measures for robust classification in sector scan sonar image sequences. IEEE Journal of Oceanic Engineering, 24(4):458–469, 1999.

[TEN01a] – I. Tena Ruiz, Y. Petillot, D. M. Lane, and C. Salson. Feature extraction and data association for AUV concurent mapping and localisation. In Proc. IEEE Internationnal Conference on Robotics and Automation (ICRA'01), Seoul, Korea, May 2001, pp. 2785–2790.

[TEN01b] – I. Tena Ruiz. Enhanced concurrent mapping and localisation using forward-looking sonar. Ph.D. dissertation, Heriot-Watt University, Edinburgh, Scotland, Sept. 2001.

[TEN03a] – I. Tena Ruiz, S. de Racourt, Y. Petillot, and D. M. Lane. Concurrent mapping & localisation using side-scan sonar. Submitted to the Journal of Oceanic Engineering, January 2003.

[TEN03b] – I. Tena Ruiz, Y. Petillot, D. M. Lane and A. Cormack. Large scale side-scan sonar Mosaics. In MREP03 Conference, La Spezia, Italy, May 2003.

[ALT01] – C. von Alt, B. Allen, T. Austin, N. Forrester, R. Goldsborough, M. Purcell, and R. Stokey, "Hunting for mines with REMUS: a high performance, affordable, free swimming underwater robot," in Proc. MTS/IEEE Internationnal Conference OCEANS'01, 2001, pp. 117–122.